J|A|C|S
ARTICLES

Published on Web 05/04/2009

Highly Ordered Self-Assembly of 1D Nanoparticles in Phospholipids Driven by Curvature and Electrostatic Interaction

Tae-Hwan Kim,[†] Shin-Hyun Kang,[†] Changwoo Doe,[†] Jihyun Yu,[†] Jun-Bo Sim,[†] Jehan Kim,[‡] Steven R. Kline,[§] and Sung-Min Choi*[,†]

Department of Nuclear and Quantum Engineering, KAIST, 373-1 Guseong-dong, Yuseong-gu, Daejeon, 305-701, Republic of Korea, Beamline Research Division, Pohang Accelerator Laboratory, Pohang University of Science and Technology, Pohang, Gyeongbuk 790-784, Republic of Korea, and NIST Center for Neutron Research, Gaithersburg, Maryland 20899-6102

Received March 9, 2009; E-mail: sungmin@kaist.ac.kr

Abstract: Self-assembly of 1D nanoparticles such as carbon nanotubes or nanorods into highly ordered superstructures using various interactions has been of great interest as a route toward materials with new functionalities. However, the phase behavior of 1D nanoparticles interacting with surrounding materials, which is the key information to design self-assembled superstructures, has not been fully exploited yet. Here, we report for the first time a new phase diagram of negatively charged 1D nanoparticle and cationic liposome (CLs) complexes in water that exhibit three different highly ordered phases, intercalated lamellar, doubly intercalated lamellar, and centered rectangular phases, depending on particle curvature and electrostatic interactions. The new phase diagram can be used to understand and design new highly ordered self-assemblies of 1D nanoparticles in soft matter, which provide new functionalities.

Introduction

Self-assembly of 1D nanoscale materials such as carbon nanotubes, nanowires, and nanorods with metallic or semiconducting properties into highly ordered superstructures has been of great interest as a route toward materials with new functional structures.[1−4] The ordered assembly of 1D nanoparticles collectively enhances their physical properties and provides a wide range of potential applications such as optoelectronic devices,[5−7] biological sensing,[8,9] and drug and gene delivery.[10,11] Recently, various techniques for assembling 1D nanoparticles into novel superstructures have been actively investigated utilizing internal interactions[12−15] or external forces.[16−18] The self-assembly of 1D nanoparticles using internal interactions such as electrostatic or hydrophobic interactions may provide a general and inexpensive way for fabricating a large variety of functional materials without going through complicated preparative procedures. However, the phase behavior of 1D nanoparticles interacting with surrounding materials, which is the key information to design self-assembled superstructures, has not been fully exploited yet.

In this article, we report a new phase diagram of negatively charged cylindrical nanoparticle and cationic liposome (CL) complexes that exhibit three different highly ordered phases, intercalated lamellar, doubly intercalated lamellar, and centered rectangular phases, depending on particle curvature and electrostatic interactions. It should be noted that, to the best of our knowledge, the centered rectangular columnar phase of 1D nanoparticle−CL complexes has not been previously reported, whereas the intercalated lamellar and the doubly intercalated

* To whom correspondence should be addressed.
† KAIST.
‡ Pohang University of Science and Technology.
§ NIST Center for Neutron Research.

(1) Kim, F.; Kwan, S.; Akana, J.; Yang, P. *J. Am. Chem. Soc.* **2001**, *123*, 4360–4361.
(2) Park, S.; Lim, J.-H.; Chung, S.-W.; Mirkin, C. A. *Science* **2004**, *303*, 348–351.
(3) Li, X.; Zhang, L.; Wang, X.; Shimoyama, I.; Sun, X.; Seo, W.-S.; Dai, H. *J. Am. Chem. Soc.* **2007**, *129*, 4890–4891.
(4) Xia, Y.; Yang, P.; Sun, Y.; Wu, Y.; Mayers, B.; Gates, B.; Yin, Y.; Kim, F.; Yan, H. *Adv. Mater.* **2003**, *15*, 353–389.
(5) Hu, J.; Li, L.; Yang, W.; Manna, L.; Wang, L.; Alivisatos, A. P. *Science* **2001**, *292*, 2060–2063.
(6) Huynh, W. U.; Dittmer, J. J.; Alivisatos, A. P. *Science* **2002**, *295*, 2425–2427.
(7) Lee, M.; Im, J.; Lee, B. Y.; Myung, S.; Kang, J.; Huang, L.; Kwon, Y.-K.; Hong, S. *Nature Nanotech.* **2006**, *1*, 66–71.
(8) Sudeep, P. K.; Joseph, S. T. S.; Thomas, K. G. *J. Am. Chem. Soc.* **2005**, *127*, 6516–6517.
(9) Huang, X. H.; El-Sayed, I. H.; Qian, W.; El-Sayed, M. A. *J. Am. Chem. Soc.* **2006**, *128*, 2115–2120.
(10) Salem, A. K.; Searson, P. C.; Leong, K. W. *Nat. Mater.* **2003**, *2*, 668–671.
(11) Gorelikov, I.; Field, L. M.; Kumacheva, E. *J. Am. Chem. Soc.* **2004**, *126*, 15938–15939.
(12) Li, L. S.; Walda, J.; Manna, L.; Alivisatos, A. P. *Nano Lett.* **2002**, *2*, 557–560.
(13) Dumestre, F.; Chaudret, B.; Amiens, C.; Respaud, M.; Fejes, P.; Renaud, P.; Zurcher, P. *Angew. Chem., Int. Ed.* **2003**, *42*, 5213–5216.
(14) Talapin, D. V.; Shevchenko, E. V.; Murray, C. B.; Kornowski, A.; Forster, S.; Weller, H. *J. Am. Chem. Soc.* **2004**, *126*, 12984–12988.
(15) Koltover, I.; Sahu, S.; Davis, N. *Angew. Chem., Int. Ed.* **2004**, *43*, 4034–4037.
(16) Harnack, O.; Pacholski, C.; Weller, H.; Yasuda, A.; Wessels, J. M. *Nano Lett.* **2003**, *3*, 1097–1101.
(17) Smith, P. A.; Nordquist, C. D.; Jackson, T. N.; Mayer, T. S.; Martin, B. R.; Mbindyo, J.; Mallouk, T. E. *Appl. Phys. Lett.* **2000**, *77*, 1399–1401.
(18) Hangarter, C. M.; Myung, N. V. *Chem. Mater.* **2005**, *17*, 1320–1324.

 10.1021/ja901810n CCC: $40.75 © 2009 American Chemical Society

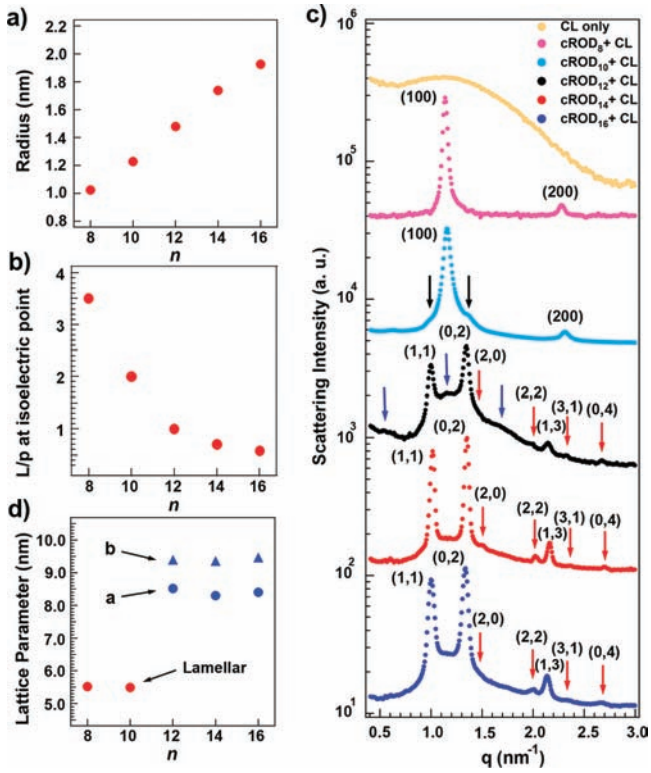

Figure 1. a) Radius of $cROD_n$. b) *L*/*p* ratio of $cROD_n$−CL complexes at isoelectric points. c) SAXS intensities of $cROD_n$−CL complexes at their isoelectric points. d) Lattice parameters obtained from SAXS analyses for complexes.

lamellar structures were observed in rodlike biomolecule−CL complexes.[19,20]

Results and Discussion

Negatively charged rodlike nanoparticles with various radii ($cROD_n$) were synthesized by copolymerization of polymerizable surfactants, *n*-alkyltrimethylammonium 4-vinylbenzoate (C_nTVB, n = the number of carbon in alkyl chain), which form wormlike micelles in water, and the anionic hydrotropic salt, sodium 4-styrenesulfonate (NaSS).[21,22] The radius and surface charge of the nanoparticles are controlled by the alkyl chain length (n = 8, 10, 12, 14, and 16) and the concentration of NaSS during copolymerization, respectively. The concentration of NaSS was maintained at 25% by mole relative to C_nTVB concentration. The structures of $cROD_n$ were characterized by small-angle neutron scattering measurements. As n is increased from 8 to 16, the radius of the particles increases from 1.0 to 1.9 nm linearly (part a of Figure 1), which is consistent with a previous study.[23] The length of the particles is nearly constant at ca. 20 nm for n = 8−14 and 41 nm for n = 16 (Supporting Information). The CLs were prepared by extruding a 5:5 (mass ratio) mixture of univalent cationic lipid, dioleoyltrimethylammoniumpropane (DOTAP), and zwitterionic lipid, dioleoylphosphatidylcholine (DOPC), through 200 nm Nucleopore filters. The $cROD_n$ and CLs were mixed in water at various mass ratios

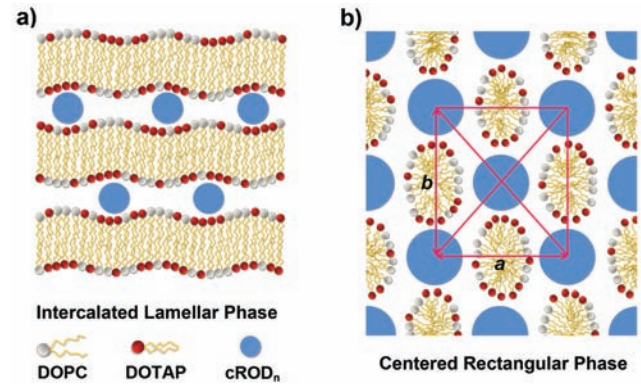

Figure 2. a) Intercalated lamellar structure of $cROD_n$−CL complex for n = 8 and 10. The $cROD_n$ may not be well ordered (text). b) Centered rectangular columnar structure of $cROD_n$−CL complex for n = 12, 14, and 16. *a* and *b* are the lattice parameters.

while the total concentration of $cROD_n$ and CL was maintained at 1.2 wt %. Dynamic light scattering and zeta potential measurements show that the mixtures form large aggregates near the isoelectric point where the zeta potential changes its sign from positive to negative (Supporting Information). As n is increased from 8 to 16, the mass ratio (*L*/*p*) of CL and $cROD_n$ at the isoelectric points decreases from 3.5 to 0.58 (part b of Figure 1), which indicates that the surface charge density of the $cROD_n$ decreases[24] with n.

The small-angle X-ray scattering (SAXS) measurements of the $cROD_n$−CL complexes were performed at 25 °C using the 4C1 beamline at the Pohang Accelerator Laboratory, Korea. The $cROD_n$−CL complexes were equilibrated for one day at room temperature before SAXS measurements. The SAXS intensities of the $cROD_n$−CL complexes at the isoelectric points and the CL only are shown in part c of Figure 1. The SAXS intensity of the CL only (25 mg/mL) shows a broad peak at q = 1.2 nm^{-1}, which is from a few stacks of lipid bilayers. On the other hand, the SAXS intensities of the $cROD_n$−CL complexes show very sharp peaks indicating highly ordered structures. It is also very interesting that as n is increased from 8 to 16, the scattering patterns change dramatically at n = 12.

For the smallest diameter $cROD_n$ (n = 8 and 10), the scattering peaks at q = 1.14 and 2.28 nm^{-1} can be indexed with (100) and (200) reflections of a multilamellar structure with alternating lipid bilayers and a $cROD_n$ monolayer, corresponding to a repeat distance of 5.5 nm (part d of Figure 1). In contrast to DNA−CL (DOPC/DOTAP) complexes,[19] however, the $cROD_n$−$cROD_n$ correlation peak was not observed, which may indicate that the $cROD_n$ are weakly ordered or randomly distributed in the water layer. Considering the lipid bilayer thickness[19] of 3.9 nm and the lamellar repeat distance of 5.5 nm, the water layer thickness of the $cROD_n$−CL complexes is 1.6 nm, which is smaller than the diameter of even the smallest $cROD_n$ particles (2.0 and 2.4 nm for n = 8 and 10, respectively). This suggests that the lipid membranes have an undulated multilamellar structure induced by the intercalated $cROD_n$ particles (part a of Figure 2). It is interesting to note that the repeat distance of $cROD_8$−CL and $cROD_{10}$−CL complexes are essentially same even though the diameters of $cROD_8$ and

(19) Rädler, J. O.; Koltover, I.; Salditt, T.; Safinya, C. R. *Science* **1997**, *275*, 810–814.
(20) Wong, G. C. L.; Tang, J. X.; Lin, A.; Li, Y.; Janmey, P. A.; Safinya, C. R. *Science* **2000**, *288*, 2035–2039.
(21) Kim, T.-H.; Choi, S.-M.; Kline, S. R. *Langmuir* **2006**, *22*, 2844–2850.
(22) Kline, S. R. *Langmuir* **1999**, *15*, 2726–2732.
(23) Gerber, M. J.; Walker, L. M. *Langmuir* **2006**, *22*, 941–948.

(24) The different molecular weight of C_nTVB accounts for about 25% decrease of the *L*/*p* ratio at the isoelectric point (when n is increased from 8 to 16), which is much smaller than the measured decrease of the *L*/*p* ratio. Therefore, the decrease of *L*/*p* ratio with n is mainly due to the decrease of surface charge density of $cROD_n$.

$cROD_{10}$ are different, which suggest that the difference in diameter may be accommodated by a different degree of undulation of the lipid bilayers. When $n = 10$, two weak additional peaks can also be observed at $q = 0.99$ and 1.34 nm^{-1} (black arrows), which increase in strength as n is increased ($n = 12$, 14, and 16). This indicates the growth of a second, topologically different structure.

In the scattering intensities of the $cROD_n$−CL complexes with $n = 12$, 14, and 16, the multilamellar peaks have almost completely disappeared[25] and a new set of sharp peaks appear, indicating a topological phase transition (part c of Figure 1). The new scattering peaks can be well indexed with a centered rectangular columnar packing to the seventh order where the peak positions occur at $2\pi\sqrt{[(h/a)^2 + (k/a)^2]}$ with the 2D lattice parameters a and b. The (h, k) peaks obey $h + k = 2m$, indicating the centered symmetry of the lattice. The lattice parameters a and b are nearly constant at 8.4 and 9.4 nm, respectively (part d of Figure 1).[26] For $n = 12$, the additional scattering peaks (three blue arrows) are observed, which will be discussed later.

To identify the detailed structure of the centered rectangular columnar packing, the various possible form factors, which determine the relative intensities of scattering peaks, were calculated and compared with the measured SAXS intensities (Supporting Information). In these calculations, the mass balance between the lipids and $cROD_n$ ($n = 14$ and 16) was maintained to match the L/p ratios at the isoelectric points. The peak intensity ratios among the first three peaks, (0,2)/(1,1) and (2,0)/(1,1), were compared with measured ratios ((0,2)/(1,1) = 1.1 and (2,0)/(1,1) = 0.069 for $n = 16$). Higher-order peaks, which are more sensitive to defects of packing order than the first three peaks, were not considered. In the centered rectangular columnar packing model (part b of Figure 2), which provides the peak intensity ratios consistent with the measured SAXS intensity ratios, the $cROD_n$ are positioned between elliptic cylindrical micelles of lipids. The thicknesses of the elliptic cylindrical micelles along the short and long axes are 2.4 and 5.1 nm (for $n = 16$), respectively. The thickness along the short axis is shorter than the bilayer thickness of DOTAP/DOPC in the lamellar phase, which can be attributed to the high curvature of the micellar interface and resulting chain packing. We expect that whereas the neutral DOPC are preferentially positioned along the short axis, the positively charged DOTAP are preferentially positioned along the long axis due to the entropy gain of the screening counterions close to positively curved micellar structures compared to planar ones.[27] In fact, this local demixing of DOTAP and DOPC may be the reason why the lipids form elliptic cylindrical micelles rather than circular ones. This anisotropy of lipid micelles leads to the formation of the centered rectangular packing rather than hexagonal packing. Another possibility for the packing structure is the inverted centered rectangular columnar packing with the $cROD_n$ at their centers. However, in this model, any combination of parameters did not satisfy the measured peak intensity ratios and the mass balance between $cROD_n$ and lipids at the isoelectric points, simultaneously. Therefore, the inverted centered rectangular columnar packing structure was discarded.

The centered rectangular columnar packing of $cROD_n$−CL complex is in contrast to the DNA−DMPC/DMTAP[28] and DNA−DPPC/calcium[29] complexes where the lamellar peaks and centered rectangular peaks are observed simultaneously, indicating an intercalated centered rectangular columnar packing of DNA. It is also in contrast to the DNA−DOPE/DOTAP complex,[30] where a transition from lamellar to a columnar inverted hexagonal phase is observed, and the F-actin−DOPC/DOTAP complexes[20] where the doubly intercalated lamellar structure (lipid bilayer−actin−actin−lipid bilayer) is observed. To our knowledge, the centered rectangular columnar packing structure of the $cROD_n$−CL complex has not been observed in any other rodlike biomolecule−CL complexes.

To understand the lamellar to centered rectangular phase transition of the $cROD_n$−CL complex with n, the radius and the surface charge density of $cROD_n$, which were changed with n simultaneously, should be considered simultaneously. When all of the $cROD_n$ are intercalated in oppositely charged multilamellar lipid membranes and form a 1D lattice, the center-to-center distance between neighboring particles ($d_{spacing}$) can be given as[19]

$$d_{spacing} = \frac{\pi d_{rod}^2 \rho_{rod}}{4\delta_m \rho_L}(L/p) \quad (1)$$

where d_{rod} is the particle diameter, δ_m is the membrane thickness, ρ_{rod} and ρ_L are the mass densities of $cROD_n$ and lipids, respectively. At the isoelectric point, $d_{spacing}$ can be expressed as $d_{spacing} = \pi d_{rod}(\sigma_{rod}/\sigma_m)$ where σ_{rod} and σ_m are the surface charge densities of $cROD_n$ and lipid membrane respectively, indicating that the interparticle distance is determined by the particle diameter and the surface charge density ratio. Because the intercalated $cROD_n$ cannot sterically overlap each other, the $d_{spacing}/d_{rod}$ ratio should be always larger than one to form the intercalated 1D lattice. Therefore, the $d_{spacing}/d_{rod}$ can be used as a criterion to determine if the $cROD_n$−CL complex forms the intercalated 1D lattice. In fact, the $d_{spacing}/d_{rod}$ ratio of the $cROD_n$−CL complexes at their isoelectric points, which was calculated by eq 1, is larger than one for $n = 8$ and 10, whereas it is smaller than one for $n = 12$, 14, and 16, which explains why the intercalated 1D lattice structure transforms into a topologically different structure at $n = 12$.

When the $d_{spacing}/d_{rod}$ calculated by eq 1 is less than one (meaning that the diameter of charged rodlike particles is too large to adjust its lattice spacing to match the membrane charge density), it is natural to form two layers of intercalated lattice of $cROD_n$ between two bilayers (a doubly intercalated lamellar structure) to maximize counterion release and entropic gain.[31−33] A simple geometrical consideration indicates that the doubly intercalated lamellar structure requires $0.5 < d_{spacing}/d_{rod} < 1$. In fact, the F-actin−DOPC/DOTAP complex, which forms the doubly intercalated lamellar structure, satisfies this condition

(25) Peak splitting indicates that the peak intensity of remaining lamellar peak at $q = 1.14$ nm^{-1} is about 8% of the (02) peak (when $n = 14$). This indicates that a small amount of lamellar phase coexists with the centered rectangular phase.

(26) When the radius of $cROD_n$ increases with n, the lattice arameters a and b are expected to increase as well. However, the lattice parameters are nearly constant. This may be attributed to the decreased L/p ratio (smaller amount of lipids) with n.

(27) May, S. *Eur. Phys. J. E* **2000**, *3*, 37–44.

(28) Artzner, F.; Zantl, R.; Rapp, G.; Rädler, J. O. *Phys. Rev. Lett.* **1998**, *81*, 5015–5018.

(29) McManus, J. J.; Rädler, J. O.; Dawson, K. A. *J. Am. Chem. Soc.* **2004**, *126*, 15966–15967.

(30) Koltover, I.; Salditt, T.; Rädler, J. O.; Safinya, C. R. *Science* **1998**, *281*, 78–81.

(31) Salditt, T.; Koltover, I.; Rädler, J. O.; Safinya, C. R. *Phys. Rev. Lett.* **1997**, *79*, 2582–2585.

(32) Koltover, I.; Salditt, T.; Safinya, C. R. *Biophys. J.* **1999**, *77*, 915–924.

(33) Koltover, I.; Wagner, K.; Safinya, C. R. *Proc. Natl. Acad. Sci. U.S.A.* **2000**, *97*, 14046–14051.

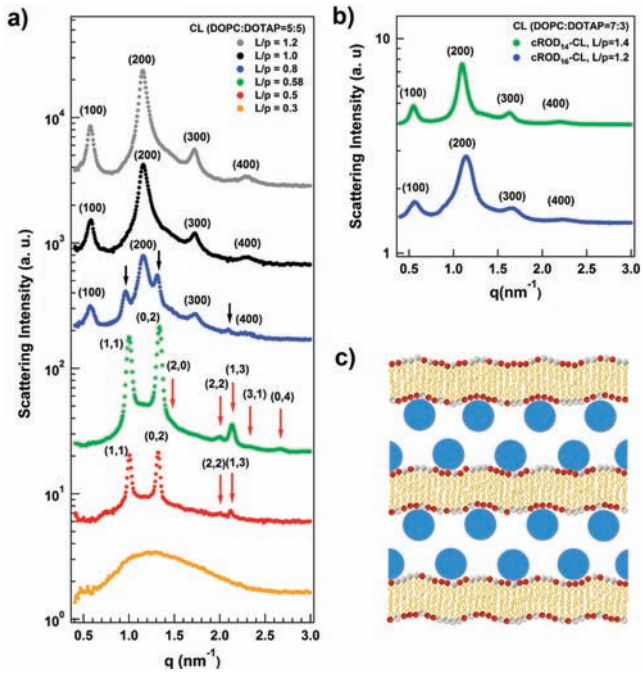

Figure 3. a) SAXS intensities of cROD$_{16}$−CL complex for different *L*/*p* ratios and DOPC/DOTAP = 5:5. b) SAXS intensities of cROD$_n$−CL complexes for n = 14 and 16 with a different CL composition of (DOPC/DOTAP = 7:3) at their isoelectric points. c) Doubly intercalated lamellar structure of cROD$_n$−CL complex for n = 14 and 16 at isoelectric points and for n = 16 at *L*/*p* = 1.0 and 1.2.

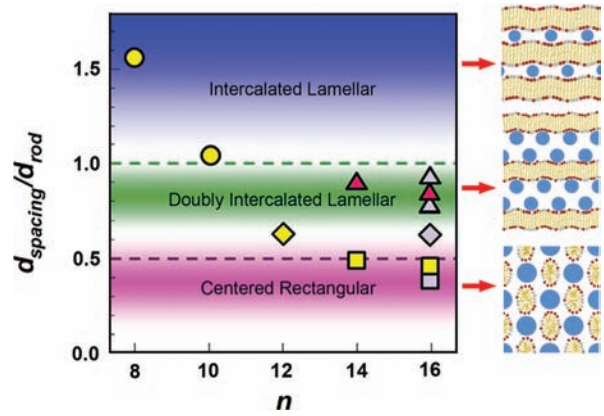

Figure 4. Phase diagram of the cROD$_n$−CL complexes in terms of the $d_{spacing}/d_{rod}$ ratio. The structures and the conditions of samples were denoted by the shape and color of the legends. Circles: intercalated lamellar structure. Triangles: doubly intercalated lamellar structure. Squares: centered rectangular structure. Diamonds: mixed phase (doubly intercalated lamellar + centered rectangular). Yellow: cROD$_n$−CL complexes (DOPC/DOTAP = 5:5) at their isoelectric points. Red: cROD$_n$−CL complexes (DOPC/DOTAP = 7:3) at their isoelectric points. Gray: cROD$_{16}$−CL complex (DOPC/DOTAP = 5:5) at nonisoelectric points (*L*/*p* = 0.5, 0.8, 1.0, and 1.2). The dotted lines are the phase boundaries expected from the $d_{spacing}/d_{rod}$ ratio.

quite well ($d_{spacing}/d_{rod}$ = 0.81). However, the cROD$_n$−CL complexes with n = 14 and 16 ($d_{spacing}/d_{rod}$ = 0.49 and 0.45, respectively) do not satisfy the condition, which clearly explains why they do not form the doubly intercalated lamellar structure. When $d_{spacing}/d_{rod} < 0.5$, the surface area of the lipid bilayers is too small to accommodate all the cROD$_n$ even if the particles are doubly intercalated, which results in incomplete counterion release. To maximize the counterion release and thereby entropic gain, the lipid bilayers rupture and reassemble into elliptic cylindrical micelles, forming the centered rectangular columnar packing together with the cROD$_n$ (n = 14 and 16). It should be noted that the cROD$_{12}$−CL complex ($d_{spacing}/d_{rod}$ = 0.62), which satisfies the condition for the doubly intercalated lamellar structure, also forms the centered rectangular structure rather than the doubly intercalated lamellar structure. However, there are additional scattering peaks indicated by three blue arrows that may indicate a mixed phase where two topologically different morphologies coexist.

To test the formation of the doubly intercalated lamellar structure in the cROD$_n$−CL complex when $0.5 < d_{spacing}/d_{rod} < 1$, the *L*/*p* ratio was varied in two different ways. In one case, while the composition of membrane was maintained (DOPC/DOTAP = 5:5), a series of cROD$_{16}$−CL complexes were prepared at different nonisoelectric points, that is different *L*/*p* ratios (0.3, 0.5, 0.58, 0.8, 1.0, and 1.2). In the other case, cROD$_n$−CL complexes (for n = 14 and 16) with a different membrane composition (DOPC/DOTAP = 7:3) were prepared at their isoelectric points. The SAXS intensities of the cROD$_{16}$−CL complex at different *L*/*p* ratios show that, as the *L*/*p* ratio increases above the isoelectric point (*L*/*p* = 0.58), a new set of 4 sharp peaks, which correspond to a lamellar structure with a repeat distance of 11.0 nm, appeared (part a of Figure 3). Considering that the bilayer thickness of DOPC/DOTAP (5:5) is 3.9 nm, the gap between two bilayers is 7.1 nm, which is almost twice the diameter of the cROD$_{16}$ (3.86 nm). Therefore, the 4 new scattering peaks can be attributed to the doubly intercalated lamellar structure (lipid bilayer−rod−rod−lipid bilayer) of the complexes (part c of Figure 3). It should be noted that the cROD$_{16}$−CL complexes with an *L*/*p* ratio above the isoelectric points satisfy the condition for the doubly intercalated lamellar structure ($d_{spacing}/d_{rod}$ = 0.62, 0.78, and 0.93 for *L*/*p* = 0.8, 1.0, and 1.2, respectively). When *L*/*p* = 0.8, the three peaks corresponding to the centered rectangular columnar structure (indicated by black arrows in part a of Figure 3) coexist with the peaks corresponding to the doubly intercalated lamellar structure, indicating a mixed phase. In fact, a similar mixed phase was observed in the cROD$_{12}$−CL complex at its isoelectric point where $d_{spacing}/d_{rod}$ = 0.62 (part c of Figure 1). When the *L*/*p* ratio was decreased below the isoelectric point, two different scattering patterns were observed. When the *L*/*p* ratio is 0.5 ($d_{spacing}/d_{rod}$ = 0.39), the cROD$_{16}$−CL complex shows a scattering pattern corresponding to the centered rectangular structure, which is same as the structure at the isoelectric point. However, when the *L*/*p* is further decreased to 0.3 ($d_{spacing}/d_{rod}$ = 0.23), the cROD$_{16}$−CL complex does not form any visible aggregates and its scattering pattern is similar to that of pure CL in water, indicating that cROD$_{16}$ are well dispersed without forming any aggregates. This indicates that the surface charge of the CL is insufficient to compensate the surface charge of cROD$_{16}$, preventing the formation of aggregates under the highly unbalanced charge condition.

The SAXS intensities of the cROD$_n$−CL complexes with a membrane composition of DOPC/DOTAP = 7:3 at their isoelectric points (for n = 14 and 16, *L*/*p* = 1.4 and 1.2, respectively) show 4 sharp peaks corresponding to lamellar structures with repeat distances of 11.4 and 11.1 nm, respectively (part b of Figure 3). Because the bilayer thickness of DOPC/DOTAP (7:3) is[34] 4.3 nm, the gaps between two bilayers are 7.1 and 6.8 nm for n = 14 and 16 respectively, which are almost twice the diameters of the cROD$_n$ (3.48 and 3.86 nm for n =

(34) Yang, L.; Liang, H.; Angelini, T. E.; Butler, J.; Coridan, R.; Tang, J. X.; Wong, G. C. L. *Nat. Mater.* **2004**, *3*, 615–619.

14 and 16, respectively), indicating the doubly intercalated lamellar structure. It should be noted that both of the $cROD_n$−CL complexes satisfy the condition for the doubly intercalated lamellar structure ($d_{spacing}/d_{rod} = 0.90$ and 0.84 for $n = 14$ and 16, respectively). The reason why the intensity of the first-order peak is smaller than that of the second-order peak can be explained by the form factor of the doubly intercalated lamellar structure, which has the maximum value near that of the second-order peak (Supporting Information). The $cROD_n$−$cROD_n$ correlation peaks in the complexes were not observed, which may indicate that the $cROD_n$ are weakly ordered or randomly distributed.

The structures of the $cROD_n$−CL complexes investigated in this study are summarized in terms of the $d_{spacing}/d_{rod}$ ratios (Figure 4), providing a new phase diagram of the $cROD_n$−CL complexes. It should be noted that all of the $cROD_n$−CL complexes follow the $d_{spacing}/d_{rod}$ ratio criteria for different complex structures (the intercalated lamellar structure ($d_{spacing}/d_{rod} > 1$), the doubly intercalated lamellar structure ($0.5 < d_{spacing}/d_{rod} < 1$), and the centered rectangular structure ($d_{spacing}/d_{rod} < 0.5$)) very well with the exception of the boundary region where mixed phases exist. Therefore, the $d_{spacing}/d_{rod}$ ratio calculated from eq 1 can be used as a simple criterion to predetermine the self-assembled superstructures of the 1D nanoparticle−CL complex. In other words, the self-assembled superstructures of 1D nanoparticle−CL complexes can be designed by controlling the diameter of the particles and the surface charge densities of the particles and membranes, which determine the $d_{spacing}/d_{rod}$ ratio.

Conclusions

We report for the first time a new phase diagram of the negatively charged 1D nanoparticle and cationic liposome complexes in water that self-assemble into three different highly ordered superstructures, the intercalated lamellar, the doubly intercalated lamellar, and the centered rectangular structures depending on the $d_{spacing}/d_{rod}$ ratio, which depends on the particle curvature and electrostatic interaction. The new phase diagram or the $d_{spacing}/d_{rod}$ ratio criterion can be used to understand and design new highly ordered self-assemblies of 1D nanoparticles, such as carbon nanotubes, in soft matter and may provide new novel routes for scalable production of ordered 1D nanoparticle composites with new functionalities. Furthermore, it may provide further insight into the interactions of rodlike biomolecules, such as DNA, with lipid membranes.

Acknowledgment. We would like to thank Prof. C. R. Safinya for useful discussions. This work is supported by the Ministry of Education, Science and Technology of Korea through the Basic Atomic Energy Research Institute (BAERI) program and the basic science research program (R-01-2008-000-10219-0).

Supporting Information Available: Materials, detailed sample preparations and characterizations, and form factor analysis. This material is available free of charge via the Internet at http://pubs.acs.org.

JA901810N